Coexistence of Two Colloidal Crystals at the Nematic-Liquid-Crystal–Air Interface

A. B. Nych,[1] U. M. Ognysta,[1] V. M. Pergamenshchik,[1] B. I. Lev,[1] V. G. Nazarenko,[1,*]
I. Muševič,[2] M. Škarabot,[2] and O. D. Lavrentovich[3]

[1]*Institute of Physics, prospekt Nauky, 46, Kiev 03039, Ukraine*
[2]*J. Stefan Institute, Jamova 39, 1000 Ljubljana, Slovenia*
[3]*Liquid Crystal Institute, Kent State University, Kent, Ohio 44242, USA*
(Received 25 September 2006; published 1 February 2007)

Glycerol droplets at a nematic-liquid-crystal–air interface form two different lattices—hexagonal and dense quasihexagonal—which are separated by the energy barrier and can coexist. Director distortions around each droplet form an elastic dipole. The first order transition between the two lattices is driven by a reduction of the dipole-dipole repulsion through reorientation of these dipoles. The elastic-capillary attraction is essential for the both lattices. The effect has a many-body origin.

Introduction.—Colloidal structures are of a continuing interest for studying general ordering phenomena in condensed matter physics [1,2]. Recently, anisotropic colloidal systems, nematic-liquid-crystal (NLC) emulsions, have been added to the field [3,4]. In NLC emulsions, the particle interactions are mediated by the elastic distortions of the unit vector field, the director **n**. Because of the anisotropy of surface interactions at the nematic-particle interface, sufficiently large (typically >0.1 μm) colloidal particles induce director distortions in the nematic sensed by other particles [5–11]. This elastic interaction is of long range and in many respects similar to the electrostatic interactions between dipoles, quadrupoles, and so on [6–11]. Particle trapping techniques [12] have been used to test this analogy and to demonstrate experimentally the dipole-dipole [13,14] and quadrupole-quadrupole [15,16] pair interactions. The useful analogy with electrostatics has enabled one to predict theoretically the basic features of few-body systems with the dipole and quadrupole interactions, namely, formation of chain structures (for a review, see [4] and references therein).

The nematic colloids also demonstrate many-body ordered structures, namely, 2D ordering of hard spheres [17] and 2D crystalline hexagonal lattices (HLs) [18] formed by glycerol droplets trapped at the NCL-air interface and stabilized by elastic-capillary interactions [19]. A glycerol droplet trapped at the interface induces director distortions of the dipole type. The elastic dipole might be either perpendicular or tilted with respect to the interface, thus leading to HLs or chain structures, respectively [19]. Dipole reorientations allow the system to explore an additional degree of freedom in the search for equilibrium. In this work, we demonstrate that by reorienting the elastic dipoles when the area per droplet is reduced, the 2D crystalline HL of glycerol droplets at the NLC-air interface can undergo a phase transition into a dense lattice (DL) with a shorter period and different symmetry. The two crystalline structures can coexist. The reverse transition can be induced by an electric field reorienting the dipoles

back to the normal state. We also demonstrate the importance of many-body effects in stabilization of the lattice: two droplets separated from the rest find themselves at distances larger than those in the DL.

Results.—The experimental setup was similar to that in [18,19]. A NLC layer (pentylcyanobiphenyl, 5CB, purchased from EM Industries) of thickness $h = 30$–100 μm is placed onto the free surface of glycerol. At the NLC-air interface, **n** is normal (homeotropic) while at the glycerol-NLC interface it is tangential, parallel to the interface. The sample is heated up to $50\,^{\circ}$C to cause diffusion of glycerol into the LC layer. Cooling down to $\sim23\,^{\circ}$C results in condensation and growth of glycerol droplets, some of which get trapped at the LC-air interface (the droplets might contain a significant amount of water absorbed from air) [19]. Their number and size can be changed by the temperature conditions (higher cooling rate produces smaller droplets). The procedure generally yields an HL [18,19], provided h is much larger than the droplet radius R (typically, 2–7 μm). In such a case the elastic dipoles induced by each droplet are practically normal to the interface despite the overall hybrid alignment of **n** in the NLC slab. The lattice vectors of HL are not related to the overall tilt of **n** and the center-to-center droplet separation D_{HL} measured along different directions is the same within about 7%. For example, within a monocrystalline area with no dislocations, containing roughly 100 droplets with $R = 2.5$ μm, we found $D_{\mathrm{HL}} \simeq 10 \pm 1$ μm, without noticeable dependence on how the lattice vector was oriented with respect to the director tilt in the NLC slab; D_{HL} was determined by averaging the data in patterns video-recorded every 6 s for 10 min.

The HL undergoes a structural phase transition into a DL when the surface area of the structure is decreased in a cone-shaped Petri dish by changing the amount of glycerol through a syringe at the bottom of the dish, Fig. 1. In a typical experiment, the initial surface area ~400 mm^2 is reduced to 300 mm^2 with a rate of 10 mm^2 per hour. During this process, one observes nucleation of islands of
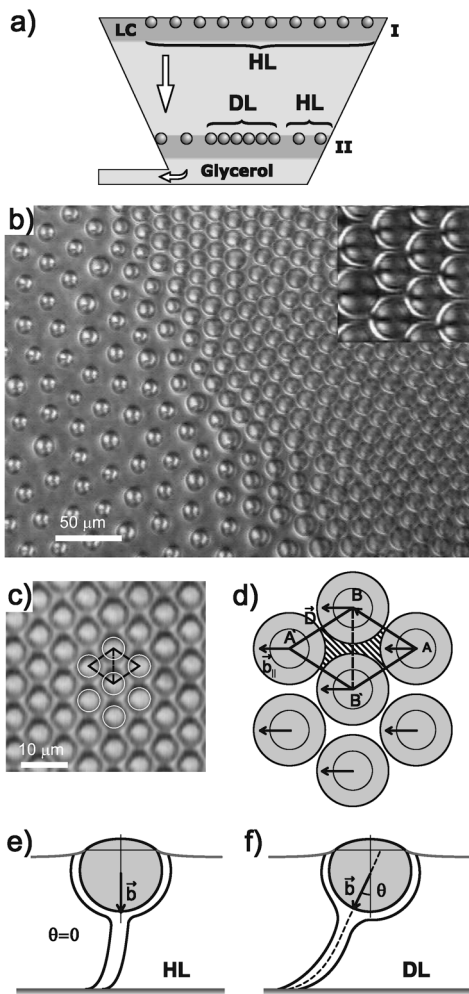
FIG. 1. HL-to-DL transition: (a) experimental setup;
(b) crossed-polarizer texture of coexisting HL and DL, inset:
magnified texture of DL; (c) magnified texture (no analyzer) of
DL and its scheme (d); elastic dipoles in HL (e) and DL (f). The
dashed in-plane projection of the director line illustrates that tilt
of **b** induces some tilt of this line on the upper NLC surface (at
the meniscus).

a new lattice, the DL, with a different symmetry and
noticeably shorter period. For example, for $R \simeq 2.5$ μm,
the typical separations are $D \simeq 6$ μm, much smaller than
$D_{HL} \simeq 10$ μm in HL. The DL is not hexagonal, as drop-
lets' separation is different along the two principal direc-
tions AB and BB', Fig. 1(c) and 1(d), with the anisotropy
parameter $\xi = (BB')/(AB) \simeq 12/11 \simeq 1.09$.

Both DL and HL are stable phases separated by the
energy barrier; they (co)exist for many days. The HL-DL
transition is irreversible: the DL areas remain stable when
the total area is increased back by adding glycerol. The
structures exist as islands disconnected from the sidewalls,
i.e., under no wall pressure, see also [19]. The reverse, DL-
HL transition, can be induced by an electric field perpen-
dicular to the lattice, Fig. 2.
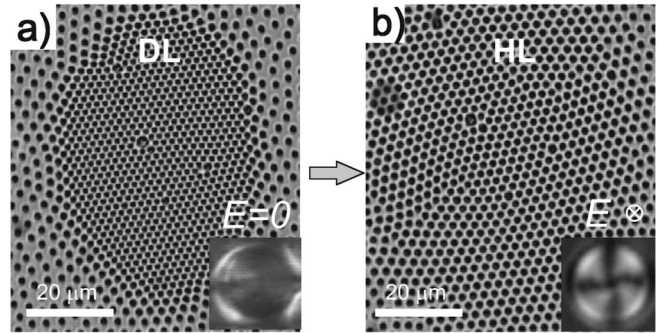
FIG. 2. DL-to-HL transition induced by the vertical electric
field $E \sim 10^4$ V/m. Insets: polarizing microscopy textures of
droplets in DL (a) and HL (b).

In the electric field experiment, we used glass substrates
with indium tin oxide (ITO) electrodes coated first by a
polymer (Elvamide 8061) film for planar alignment and
then by a 50 μm thick layer of 5CB. The glycerol droplets
were formed by condensation on the plate kept upside
down above the vessel with heated glycerol. The DLs
appear if a sufficient number of droplets is condensed,
Fig. 2(a). The second ITO electrode plate was placed
near the free surface in air as to make a gap of 0.5 mm.
5CB is of a positive dielectric anisotropy and thus the field
reorients **n** parallel to itself. The electric voltage $\sim$250 V,
1 kHz is applied across the gap. It sets the elastic dipoles
normal to the interface: the texture of each droplet be-
comes clearly axially symmetric with four extinction
brushes emerging from its center, Fig. 2(b). This dipole
reorientation is accompanied by repulsion of the droplets
within the DL, and the DL, Fig. 2(a), transforms into an HL
with a much larger period, Fig. 2(b).

The electric field experiments also demonstrate that the
many-body effects might be essential in the stability of
lattices. The electric field applied along the NLC layer
forces the droplets to approach each other at distances of
the order of AB or even smaller, Fig. 3. In this way, two
droplets well separated from the others were brought to-
gether, but as soon as the field was switched off the droplets
always moved away from each other and established their
positions at distances noticeably larger than D in the
equilibrium DL. Thus, two droplets repel each other at
distances D whereas many droplets form stable lattices
with the period D.

Discussion.—The director distortion around the droplet,
Fig. 1(e) and 1(f), is of the elastic dipole type, with the axis
b. The interaction energy of two parallel elastic dipoles is
[4]

$$U \simeq \alpha K R^4 (1 - 3\cos^2\psi)/D^3, \qquad (1)$$

where K is the elastic constant, ψ is the angle made by **b**
and the center-to-center vector **D**, Fig. 1(d), $D = |\mathbf{D}|$, and
the coefficient α [19] depends on the specific geometry of
distortions. For normally anchored inclusions, Eq. (1) is
confirmed experimentally [13,14].
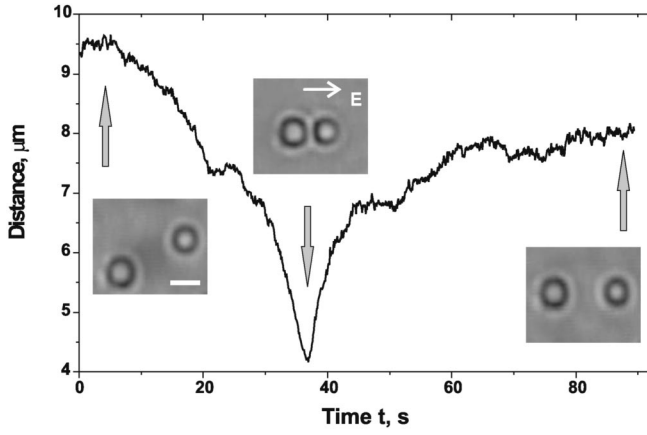
FIG. 3.   Time dependence of the center-to-center distance between two 3 μm droplets. The horizontal electric field, $E = 8 \times 10^4$ V/m, is turned on at $t = 0$ to bring the droplets together and turned off at $t = 37$ s, causing repulsion. Scale bar on first image is 3 μm.

In the HL, **b** is vertical, $\psi = \pi/2$, and U describes repulsion. The stabilizing force in the HL has the elastic-capillary nature [19]. It is known that a vertical force on colloids trapped at a liquid surface disturbs this surface, which results in a logarithmic attraction [20]. A colloid on a nematic surface induces director distortions that, trying to weaken themselves, push the colloid vertically thus giving rise to the elastic-capillary attraction. The attraction energy of two droplets scales as $\gamma_C R^2 \ln(D/\lambda)$, where $\lambda \simeq 2$ mm is the capillary length; $\gamma_C = \frac{1}{2} W_{NG}^2/\sigma_{NA}$ has the dimension of a surface tension where W_{NG} is the anchoring coefficient for the 5CB-glycerol interface and σ_{NA} is the surface tension of the 5CB-air interface [19]. For $R = 3$ μm, the equilibrium period is $D_{HL} \simeq 5R$ and the attraction energy $\sim 160kT$ [19]. For smaller D this attraction cannot compete with the repulsion $\sim 1/D^3$. However, rotation of the elastic dipoles can reduce the repulsion thus reducing the lattice period in DL as compared to HL.

Let all **b**'s make an angle θ with the layer normal and lie in the vertical plane [along AA', Fig. 1(d)]. In the hexagonal geometry, $\cos^2\psi$ in (1) for the pair AB obtains as $\cos^2\psi = (3/4)\sin^2\theta$, and a sufficiently large tilt $\theta \simeq 0.72$ can even alter the sign of U from repulsion to attraction. For $\theta > 0$, the director at the NLC-air interface will also tilt, Fig. 1(f), resulting in the anchoring energy loss proportional to the anchoring strength W at this interface and the interface area occupied by the lattice. Finally, it is seen from Fig. 1(d) and 1(f) that there is a geometrical restriction on θ. To turn by $\theta \sim \pi/2$, the end of the elastic dipoles (where the maxima of elastic distortions are concentrated) must find itself in a very restricted volume bounded by the two neighboring droplets. In this small gap the director gradients should increase sharply. Hence the dipole tilt cannot be larger than some θ_m; we assume $\theta_m \sim 1$.

A lattice of a large number N of droplets consists of N similar elementary rhombs $AB'A'B$, Fig. 1(d) in which

$AB' = D$ and $BB' = \xi D$. The elastic, anchoring, and capillary energy contained in the cell is the sum of four halves of the interaction energy between A and B, the interaction energy between B and B', and the anchoring energy for the area of the NLC-air surface free of the droplets (interaction between A and A' screened by the droplets B and B' is neglected). Then, regarding for the anisotropy ξ and introducing the dimensionless distance $r = D/R \geq 2$, the energy F of the single rhomb can be written in the form

$$\frac{F}{\alpha KR} = \frac{1}{(\xi r)^3} + \frac{2}{r^3}[1 - 3\sin^2\theta(1 - \xi^2/4)]$$

$$+ \frac{\gamma_A WR}{2K}(\sqrt{1 - \xi^2/4}\alpha r^2 - \pi\sin^2\theta)\sin^2\theta + \frac{\gamma_C R}{K}$$

$$\times \left[2\ln\left(\frac{rR}{\lambda}\right) + \ln\left(\frac{\xi rR}{\lambda}\right)\right]. \qquad (2)$$

A finite tilt θ does not change the dipole-dipole repulsion in the BB' direction [the first term in (2)], but does reduce that in the AB direction (the second term),
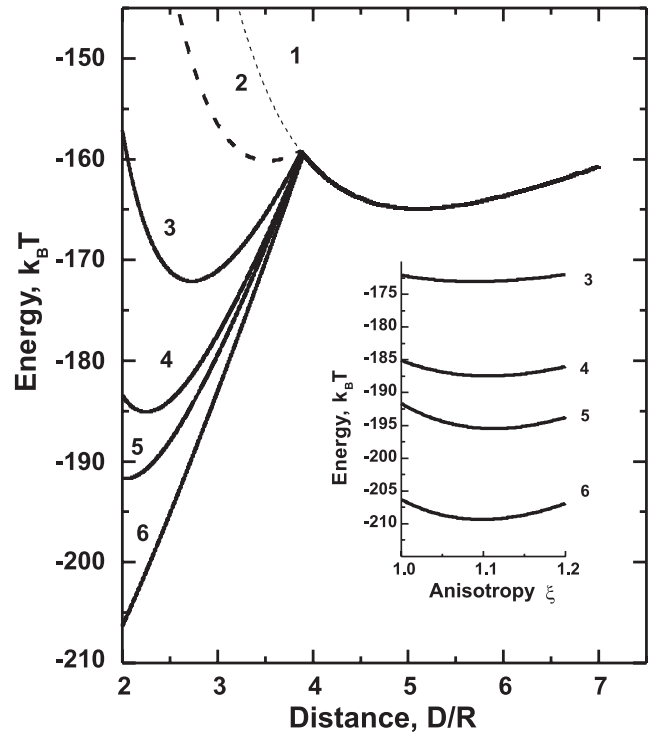
FIG. 4.   Equilibrium free energy (FE) of the lattice structure per single rhomb $BAB'A'$ vs distance r for different θ_m. $K = 7$ pN, $h = 30$ μm, $R = 3$ μm, $W = 10^{-5}$ J m^{-2}. Rightward the pick at $r_B = 3.9$, $\theta = 0$; minimum at $r \simeq 5$ corresponds to HL. Leftward the pick at $r_B = 3.9$, $\theta = \theta_m$, the minima correspond to DL: 1. $\theta_m = 0$ (the dot extension to $r < r_B$ shows the FE for $\theta = 0$); 2. $\theta_m = 0.55$ (appearance of the second minimum); 3. $\theta_m = 0.75$ ($r_{DL} = 2.7$); 4. $\theta_m = 0.83$ ($r_{DL} = 2.24$); 5. $\theta_m = 0.855$ ($r_{DL} = 2.0$ for the first time); 6. $\theta_m = 0.9$ ($r_{DL} = 2$). Inset: FE minimum $F(r_{DL}(\theta_m), \theta_m, \xi)$ vs anisotropy ξ for the curves 3–6.

giving rise to the anisotropy in the tilted phase. The third term $\propto \gamma_A W r^2 \sin^2\theta$ is that of anchoring at the nematic-air interface, written in Rapini-Papoular form, where the coefficient $\gamma_A \lesssim 1$ takes into account that the actual orientation of **b** is different from that of **n**. For large r the surface anchoring is large if $\theta \neq 0$, and F is minimum for $\theta = 0$ which is the case of HL. For small r, however, the capillary attraction and the tilt-induced reduction of repulsion can take over the anchoring energy loss. This picture is confirmed by our calculation. We minimized F for $K = 7$ pN, $W = 10^{-5}$ J m^{-2} [21], $\alpha = 0.1$, and $R = 3$ μm. The results can be described as following. If the upper bound of the tilt $\theta < \theta_c \approx 0.55$, then F is minimized by $\theta = 0$ and $\xi = 1$. The curve $F(r, \theta = 0, \xi = 1)$ has a single minimum which takes the experimental value $r_{HL} = 5$ if $\gamma_C = 5.6 \times 10^{-8}$ J m^{-2}. Thus, if $\theta < \theta_c$, the only possible lattice is HL. If, however, $\theta > \theta_c$, then $F(r, \theta, \xi)$ shows two minima, corresponding to DL with $\theta > 0$ and HL with $\theta = 0$, separated by the energy barrier at $r_B \simeq 3.9$. Below we describe the results for this case $\theta > \theta_c$, Fig. 4, setting $\gamma_A = 0.2$ for illustrative purposes (the results are similar in a wide range of $\gamma_A W$).

For any $r > r_B$, F is minimum for $\theta = 0$ and no anisotropy, $\xi = 1$; U (1) is maximum repulsive for all droplets, the anchoring term is zero. Here the curve $F(r, \theta = 0, \xi = 1)$ has a minimum at $r_{HL} \simeq 5$ which corresponds to the HL reported in [18,19]. For $2 < r < r_B$, F is minimum for the largest possible tilt $\theta = \theta_m$ and $\xi > 1$; the curve $F(r, \theta = \theta_m, \xi)$ has another minimum at some $r_{DL}(\theta_m)$ and $\xi = \xi(\theta_m)$. Depending on θ_m, this r_{DL} can vary from $r_c \simeq 3.9$ for $\theta_m \sim \theta_c = 0.55$ to 2.24 for $\theta_m = 0.83$, and, finally, to its minimum value 2 for all $\theta_m \gtrsim 0.855$. For fixed $r_{DL}(\theta_m)$, $F(\xi)$ has a minimum at $\xi_m \sim 1.1$ (Fig. 4, inset) close to the experimental value. The above picture is in agreement with the experiment: it explains the existence of HL for large r and DL for small r. The HL is separated from the DL by the barrier $\sim 10^{-3} KR \simeq 5.6 k_B T$ per droplet, while the depth of the DL minimum relative to this barrier is about $\sim 4 \times 10^{-3} KR \simeq 23 k_B T$ for $\theta_m \sim 1$. The depth of the fine minimum due to the anisotropy is about $4 \times 10^{-4} KR \simeq 2.3 k_B T$. The capillary attraction is necessary for the both lattices as for $\theta_m < 0.96$, U still describes the repulsion [i.e., the sum of the first two terms in (2) decreases with r].

Note, that in shallow systems with small thickness $h \sim R$, the tilt at the upper nematic surface is already induced by the planar boundary condition on the lower 5CB-glycerol interface. Then linear chains of droplets become those of the minimum energy and are indeed observed in thin NLC layers [19]. In thick 5CB films, the droplets form 2D lattices and do not form linear structures. A structure of N particles is energetically favorable if the energy gain $E \sim N$ due to its formation prevails the boundary energy loss $E_B \sim$ perimeter of the structure. The surface **n** within DL areas with $\theta \neq 0$ is tilted whereas outside it is not, and there is a band along the perimeter where the tilt is relaxing. For round shaped structures $E_B \sim \sqrt{N}$, and if N is large then $E_B \ll E$. This inequality is impossible for a linear structure as its perimeter $\sim N$, and $E_B \sim E$. Thus, the tilted phase is energetically favorable in more or less round islands which is a many-body effect as it requires sufficiently large N.

Conclusion.—Nematic emulsions represent a unique colloidal system with rich ordering phenomena and diverse long range interactions. Using colloids of particular shape and varying their orientational properties in principle allows one to model different types of multipole interactions. We have demonstrated one more unique advantage of the nematic emulsions: they can be used to study a coexistence and mutual transformation of crystalline phases. The strength and symmetry of elastic distortions can be changed by changing the area per particle or by applying the electric field, thus allowing one to switch between the two lattices, HL and DL.

*Electronic address: vnazaren@iop.kiev.ua

[1] P. N. Pusey, in: *Liquids, Freezing, and the Glass Transition*, edited by J. P. Hansen, D. Levesque, and J. Zinn-Justin (North-Holland, Amsterdam, 1991).

[2] K. Zahn *et al.*, Phys. Rev. Lett. **90**, 155506 (2003).

[3] P. Poulin *et al.*, Science **275**, 1770 (1997); J. Ch. Loudet, P. Barois, and P. Poulin, Nature (London) **407**, 611 (2000).

[4] H. Stark, Phys. Rep. **351**, 387 (2001).

[5] S. L. Lopatnikov and V. A. Namiot, Zh. Eksp. Teor. Fiz. **75**, 361 (1978) [Sov. Phys. JETP **48**, 180 (1978)].

[6] S. Ramaswamy *et al.*, Mol. Cryst. Liq. Cryst. **288**, 175 (1996).

[7] B. I. Lev and P. M. Tomchuk, Phys. Rev. E **59**, 591 (1999).

[8] R. W. Ruhwandl and E. M. Terentjev, Phys. Rev. E **55**, 2958 (1997).

[9] O. Kuksenok *et al.*, Phys. Rev. E **54**, 5198 (1996).

[10] T. C. Lubensky *et al.*, Phys. Rev. E **57**, 610 (1998).

[11] B. I. Lev *et al.*, Phys. Rev. E **65**, 021709 (2002).

[12] I. Muševič *et al.*, Phys. Rev. Lett. **93**, 187801 (2004).

[13] M. Yada, J. Yamamoto, and H. Yokoyama, Phys. Rev. Lett. **92**, 185501 (2004).

[14] I. I. Smalyukh *et al.*, Appl. Phys. Lett. **86**, 021913 (2005).

[15] I. I. Smalyukh *et al.*, Phys. Rev. Lett. **95**, 157801 (2005).

[16] J. Kotar *et al.*, Phys. Rev. Lett. **96**, 207801 (2006).

[17] I. Muševič *et al.*, Science **313**, 954 (2006).

[18] V. G. Nazarenko, A. B. Nych, and B. I. Lev, Phys. Rev. Lett. **87**, 075504 (2001).

[19] I. I. Smalyukh *et al.*, Phys. Rev. Lett. **93**, 117801 (2004).

[20] D. Y. C. Chan, J. D. Henry, and L. R. White, J. Colloid Interface Sci. **79**, 410 (1981).

[21] O. D. Lavrentovich and V. M. Pergamenshchik, Phys. Rev. Lett. **73**, 979 (1994).